.

Modeling of transport phenomena in tokamak plasmas with neural networks

O. Meneghini' , C. J. Luna, S. P. Smith, and L. L. Lao

Citation: Phys. Plasmas **21**, 060702 (2014); doi: 10.1063/1.4885343
View online: http://dx.doi.org/10.1063/1.4885343
View Table of Contents: http://aip.scitation.org/toc/php/21/6
Published by the American Institute of Physics

PHYSICS OF PLASMAS 21, 060702 (2014)

Modeling of transport phenomena in tokamak plasmas with neural networks

O. Meneghini,[1,a)] C. J. Luna,[2] S. P. Smith,[3] and L. L. Lao[3]
[1]*Oak Ridge Associated Universities, 120 Badger Ave, Oak Ridge, Tennessee 37830, USA*
[2]*Arizona State University, 411 N. Central Ave, Phoenix, Arizona 85004, USA*
[3]*General Atomics, San Diego, California 92186-5608, USA*

(Received 14 April 2014; accepted 11 June 2014; published online 23 June 2014)

A new transport model that uses neural networks (NNs) to yield electron and ion heat flux profiles has been developed. Given a set of local dimensionless plasma parameters similar to the ones that the highest fidelity models use, the NN model is able to efficiently and accurately predict the ion and electron heat transport profiles. As a benchmark, a NN was built, trained, and tested on data from the 2012 and 2013 DIII-D experimental campaigns. It is found that NN can capture the experimental behavior over the majority of the plasma radius and across a broad range of plasma regimes. Although each radial location is calculated independently from the others, the heat flux profiles are smooth, suggesting that the solution found by the NN is a smooth function of the local input parameters. This result supports the evidence of a well-defined, non-stochastic relationship between the input parameters and the experimentally measured transport fluxes. The numerical efficiency of this method, requiring only a few CPU-μs per data point, makes it ideal for scenario development simulations and real-time plasma control. © *2014 AIP Publishing LLC*. [http://dx.doi.org/10.1063/1.4885343]

Over the past 50 yr, there has been remarkable progress in understanding the physics underlying transport phenomena in tokamak plasmas, which has culminated in the development of sophisticated neoclassical and gyrokinetic simulation codes. Although these first principles models have been successful at describing core plasma transport in some regimes, they are computationally challenging, and are generally less accurate at the plasma edge.[1] Reduced theory-based models,[2] although significantly faster, are still computationally expensive for the purpose of full transport simulations, and can only reproduce the results of gyrokinetic models. Conventional empirical models and power scaling laws,[3,4] although easy to implement and interpret, are limited to a particular regime of operations and/or to the prediction of global plasma parameters. This motivates continued efforts to develop new transport models and improve existing ones.

In this paper, we advance the idea of using a neural network (NN) as a means to perform a nonlinear multivariate regression of transport fluxes as a function of a set of dimensionless plasma parameters. We note that in the field of magnetic fusion, NNs have also been successfully applied to other problems, including the prediction of the onset of plasma disruptions,[5,6] real time control systems,[6,7] and global confinement scaling laws.[8] Other learning approaches have also been reported.[9]

For our study, we use a multi-layer feed-forward NN topology, as shown in Fig. 1. In this NN topology, information travels from one layer of "input" neurons, through multiple layers of "hidden" neurons, and out of one layer of "output" neurons. The formalism behind this type of NN is well established.[10,11]

We assume transport to be a local phenomenon, meaning that fluxes at one radial location only depend on plasma parameters at that same radial location. This assumption is reflected in the topology of the NN, which has only one neuron for each of the input/output quantities. This should be contrasted to a global transport assumption, which would require multiple neurons for each input/output quantity for the NN to have knowledge of the plasma parameters at multiple locations across the plasma radius. In general, this assumption is satisfied by turbulent and neoclassical transport phenomena at sufficiently small Larmor radii, but not by MHD instabilities (which have a large radial extent) or by "action at a distance" phenomena.[12]

The outputs of the NN are the conductive heat fluxes defined as $Q_{e,i} = \frac{1}{S}\int_0^r q_{e,i}\, dV$, where $q_{e,i}$ are the power densities for electrons and ions, and dV and S are the flux surfaces differential volume and surface area. The NN inputs are a set of local dimensionless plasma parameters which are similar to the ones used in calculating neoclassical and turbulent fluxes from first-principles models, as listed in Table I. Here, $L_x = -\dot{x}/x = -\frac{1}{x}\frac{\partial x}{\partial r}$ is the scale length of a quantity x; c_s is the ion sound speed; ρ_i is the ion gyroradius; and r and a are the plasma minor radius and its value at the last closed flux surface, respectively. The minor radius is defined as $r = \sqrt{\Phi/\pi B_{t0}}$, where Φ is the toroidal magnetic flux, and B_{t0} is the vacuum toroidal field at a nominal major radius R_0.

The choice of an optimum network topology is a trial-and-error problem that has no closed form solution.[13] Following the well established procedure of dividing the data into three sub-sets (training, validation, and testing),[11] we systematically varied the number of hidden layers and neurons per layer (up to 4 layers of 50 neurons each), and found that 3 hidden layers of 30 neurons each consistently converged to lower training and validation errors. Simpler network topologies resulted in higher errors, while more

a)meneghini@fusion.gat.com

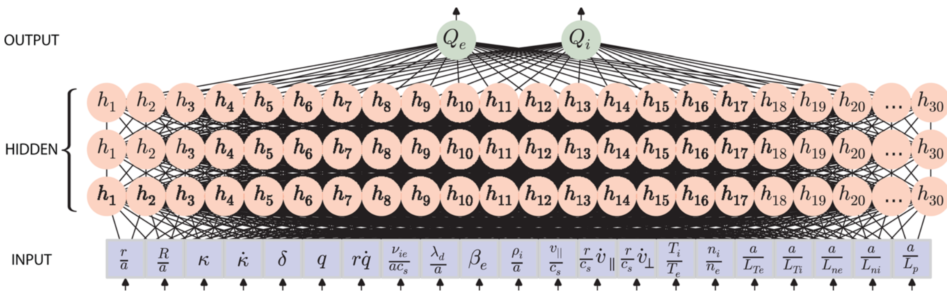

FIG. 1. Schematic of the neural network topology used to predict the electron and ion heat fluxes.

complex ones had difficulty converging. The validation error was observed to closely follow the training error, indicating that—within the range of tested topologies—the NNs do not over-fit the training data.

Given a NN topology, the behavior of the NN is governed by the connection weights among its neurons. A training process adjusts the values of the weights by minimizing the error between the NN output and the desired response to a set of known input signals, as a function of the error derivative of the weights of each neuron. For our purposes, the gradient-descent algorithm with momentum[14] is used as the learning rule and the back-propagation algorithm[15] is used to calculate error gradients at each layer.

To train the network, we make use of the vast database of ONETWO[16] experimental power-balance analyses which are run after each successful DIII-D shot (autoONETWO). ONETWO uses a fluid representation to describe the evolution of plasma quantities over transport time-scales. Axisymmetry is assumed and plasma observables are averaged on a flux surface to obtain a set of one dimensional time-dependent equations for each plasma species.

For the purpose of the autoONETWO analyses, the kinetic profiles are time-averaged over a long time interval ($\pm$20 ms) and MHD events such as sawteeth, edge localized

TABLE I. Local dimensionless plasma parameters which are input to the neural network.

r/a	$\rightarrow$	Normalized minor radius
R/a	$\rightarrow$	Normalized major radius
κ	$\rightarrow$	Elongation
$r\dot{\kappa}$	$\rightarrow$	Normalized elongation shear
δ	$\rightarrow$	Triangularity
q	$\rightarrow$	Safety factor
$r\dot{q}$	$\rightarrow$	Normalized safety factor shear
$\nu_{ie}/a/c_s$	$\rightarrow$	Normalized electron-ion collision frequency
λ_d/a	$\rightarrow$	Normalized Debye length
β_e	$\rightarrow$	Kinetic to magnetic pressure ratio
ρ_i/a	$\rightarrow$	Normalized ion gyroradius
$v_\parallel/c_s$	$\rightarrow$	Normalized parallel velocity
$r\dot{v}_\parallel/c_s$	$\rightarrow$	Normalized parallel velocity shear
$r\dot{v}_\perp/c_s$	$\rightarrow$	Normalized $E \times B$ velocity shear
T_i/T_e	$\rightarrow$	Ion to electron temperature ratio
n_i/n_e	$\rightarrow$	Ion to electron density ratio
a/L_{Te}	$\rightarrow$	Electron temperature scale length
a/L_{Ti}	$\rightarrow$	Ion temperature scale length
a/L_{ne}	$\rightarrow$	Electron density scale length
a/L_{ni}	$\rightarrow$	Ion density scale length
a/L_p	$\rightarrow$	Total pressure scale length

modes (ELMs), and toroidal Alfvén eigenmodes (TAEs) are not taken into consideration. The equilibrium reconstructions used are constrained by motional Stark effect measurements. We retain only autoONETWO time slices with no measured MHD activity (n = 1, 2, 3 modes) and for which all the input parameters are available. To avoid issues with equilibrium metrics and the transport coefficient being ill defined at the plasma edge, the NN training data are limited to $r/a \leq 0.95$. To limit the amount of data, a random subset of valid time-slices is selected and the autoONETWO 201 point radial resolution profiles are sub-sampled to 21 points uniformly distributed in r. The autoONETWO code and the analyses, on which autoONETWO depends, are automatic and therefore not immune to inaccuracies and errors. Nonetheless, these automatic workflows do a fair job at reproducing the behavior of the core heat fluxes that one would obtain by manual analyses and provide a valid basis for ensemble studies such as the one carried out in this paper.

Once the relationship between the inputs and outputs is found on a training dataset, the NN can be used to compute the output for similar inputs (a process referred to as generalization). To illustrate the NN efficiency and its ability to capture the experimentally observed heat transport, we trained the NN on DIII-D data from the 2012 campaign (809 shots; 13 993 time slices; 293 853 data points) to predict data from the 2013 campaign (1 247 shots; 22 012 time slices; 462 252 data points).

The regression plots in the left panel of Fig. 2 compare on a log scale the heat fluxes which are output by the NN and the experiments, showing good agreement over more than three orders of magnitude. On the right, histograms of the relative error (defined as $\epsilon = (Q_{\rm NN} - Q_{\rm EXP})/Q_{\rm EXP}$) normalized to the total number of points highlight the good statistical agreement of the NN model. The NN training error is observed to be mostly symmetric and is statistically smaller than the prediction error. The training error provides an estimate upper bound to what would be the best possible result that could be attained by any model using the set of input parameters and the experimental data in hand. Interestingly, the prediction error has some skewness in the distribution, which may be symptomatic of systematic changes that may have occurred between the 2012 and 2013 campaigns (e.g., different operational regimes, diagnostic calibrations, and data processing). Table II summarizes the NN regression error statistics seen in Fig. 2: transport is over predicted by less than 8% on average (4% median) and the average error remains below 30% (20% median). Training the NN only on L-mode or H-mode data showed minimal difference in the

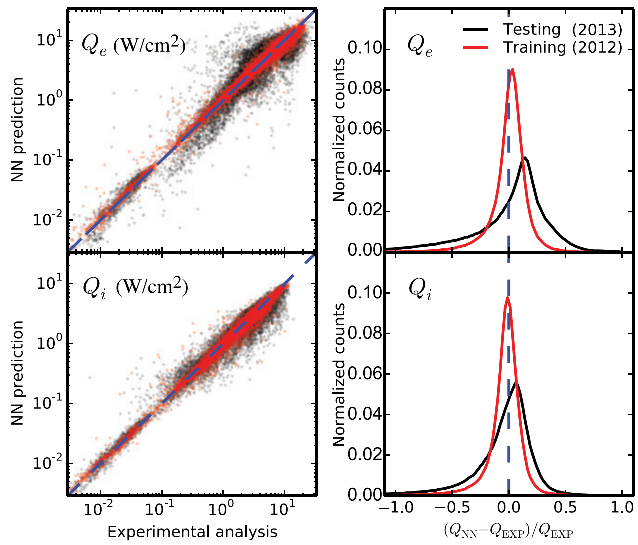

FIG. 2. On the left, regression plots compare the electron and ion heat fluxes from the NN and the experiment. On the right, histograms (100 bins ranging ± 1) show the relative error normalized to the total number of data points. The 2012 training data are in red and the 2013 testing data in black.

training error distribution ($<\pm 1\%$ in the median statistics), indicating that indeed a single NN can capture the non-linear relationship between the input parameters and output fluxes in the two regimes, and suggesting that the observed error is mostly determined by the experimental uncertainties in the data that are fed to the NN.

Multi-layer networks generalize well within the range of inputs for which they have been trained, but they cannot reliably extrapolate beyond this range, which generally result in large prediction errors. Few points from the 2013 data are affected by this issue, as it can be seen in the regression and histogram plots, and the high ratio between the mean and median errors (the median is less sensitive to outliers). The issue is likely to be alleviated as more data are used for training the NN (for example, combining the 2012 and 2013 datasets to make predictions for the 2014 campaign). Since in the experiments, the operational envelope is generally expanded in small progressive increments, one can foresee a NN model that is retrained when new operational boundaries are reached, while still providing reliable guidance up to that point.

Figure 3 shows that the NN predictions of the electron and ion heat flux profiles are in good agreement with the measurements during both steady state and transients phases

TABLE II. Percentage statistics of the relative error and its magnitude for both the training and testing data. The mean and median of the error ($\bar{\epsilon}$ and $\tilde{\epsilon}$) measure the skewness in the distribution, while the mean and median of the error magnitude ($\overline{|\epsilon|}$ and $\widetilde{|\epsilon|}$) measure its broadness.

	Training data (2012)				Testing data (2013)			
	Mean		Median		Mean		Median	
	$\bar{\epsilon}$	$\overline{\lvert\epsilon\rvert}$	$\tilde{\epsilon}$	$\widetilde{\lvert\epsilon\rvert}$	$\bar{\epsilon}$	$\overline{\lvert\epsilon\rvert}$	$\tilde{\epsilon}$	$\widetilde{\lvert\epsilon\rvert}$
Q_e	−0.6	11.8	1.9	7.4	−7.0	29.8	7.7	19.7
Q_i	−4.0	10.7	−1.7	6.5	−8.2	21.4	0.1	12.3

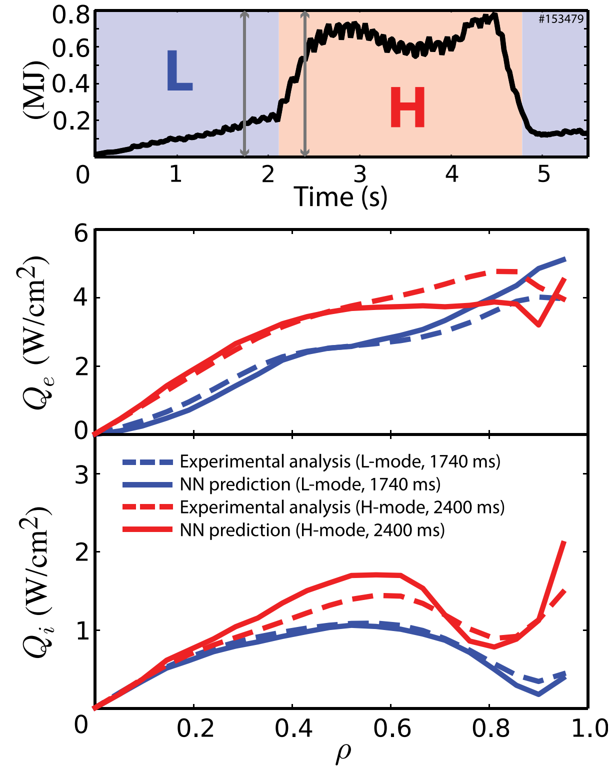

FIG. 3. Sample comparison of the electron and ion heat flux profiles from the 2013 experimental campaign and predicted by the NN. The profiles predicted by the NN are smooth and agree well with the measurements across the whole plasma radius for both H and L plasma phases.

of the L and H-mode regimes. Furthermore, it is shown that although in the model each radial location is calculated independently from the others, the heat flux profiles are smooth, suggesting that the solution found by the NN is a smooth function of the input parameters.

With the NN approach, each data point is calculated in $\sim$10 CPU-μs: about 10^5 times faster than reduced models ($\sim$1 CPU-s) and 10^{12} times faster than local gyrokinetic simulations ($\sim 10^4$ CPU-h). Such high efficiency opens exciting new possibilities for scenario development simulations and real-time plasma control.

In summary, a new model for the prediction of local heat fluxes has been developed. The model uses NN to perform an efficient non-linear multivariate regression of local transport fluxes as a function of a set of local dimensionless plasma parameters. Its capabilities have been demonstrated by training the NN on DIII-D experimental data and making predictions for an entire campaign worth of data. Results show that the predicted heat flux profiles compare quantitatively well with experimental observations across the whole plasma radius and for a broad range of plasma regimes. Overall, it can be said that the NN approach trades physical understanding of first-principle models for accuracy and speed.

The NN approach described in this paper does not make any simplifying assumption about the functional form of the underlying transport physics, besides locality; the success of this model supports the validity of the local transport hypothesis. Furthermore, the profiles predicted by the NN are smooth, which supports the evidence of a well-defined, non-stochastic relationship between the input parameters and the transport fluxes, which in principles could be captured by first principles models. In this respect, the error on the training data provides an upper bound to what would be the best possible result that could be attained by any model using the experimental data in hand.

Future prospects include identification of the most important subset of input parameters; extension to predict density and momentum fluxes; training on databases from different devices; and inclusion of the NN model in a transport code. Concerning the limited ability of a NN to predict outside of the training data range, one should notice that plasmas in DIII-D and other existing experiments can be made to match most local dimensionless parameters of larger future devices such as ITER, with the notable exception of ρ_i/a (so called *similar discharges*[17]). Hence, we speculate that prediction of future devices could be obtained by assuming that the fluxes scale in a known way with respect to ρ_i/a (e.g., $(\rho_i/a)^{-2}$ for Bohm and $(\rho_i/a)^{-3}$ for Gyro-Bohm scalings[17]). With such an assumption, one could omit ρ_i/a from the set of input parameters, train the NN on existing machines for the fluxes normalized to the known functional scaling of ρ_i/a, and apply the NN predictions to future devices. Following the idea outlined in Sec. S5 of Ref. 8, a modified NN topology and a multi-machine database could be used to infer the proper exponent of a power law ρ_i/a scaling assumption.

For this study the workflow for fetching the data, creating and training the network, and postprocessing the results is implemented as part of the OMFIT[18] integrated modeling framework. The NN itself was implemented with the FANN[19] library.

Work was supported in part by the U.S. Department of Energy under DE-FG02-95ER54309. The authors thank C. Holland, J. Candy, R. E. Waltz, O. Izacard, and S. Shiraiwa for useful discussions and X. Lee and R. Prater for their support with the autoONETWO database.

[1]T. L. Rhodes, C. Holland, S. P. Smith, A. E. White, K. H. Burrell, J. Candy, J. C. DeBoo, E. J. Doyle, J. C. Hillesheim, J. E. Kinsey, G. R. McKee, D. Mikkelsen, W. A. Peebles, C. C. Petty, R. Prater, S. Parker, Y. Chen, L. Schmitz, G. M. Staebler, R. E. Waltz, G. Wang, Z. Yan, and L. Zeng, Nucl. Fusion **51**, 063022 (2011).
[2]G. M. Staebler, J. E. Kinsey, and R. E. Waltz, Phys. Plasmas **14**, 055909 (2007).
[3]J. W. Connor, Plasma Phys. Controlled Fusion **30**, 619 (1988).
[4]ITER Physics Basis Editors, ITER Physics Expert Group Chairs and Co-Chairs and ITER Joint Central Team, and Physics Integration Unit, Nucl. Fusion **39**, 2137 (1999).
[5]C. G. Windsor, G. Pautasso, C. Tichmann, R. J. Buttery, T. C. Hender, JET EFDA Contributors, and the ASDEX Upgrade Team, Nucl. Fusion **45**, 337 (2005).
[6]A. Murari, J. Vega, D. Mazon, G. Ratta, M. Gelfsa, A. Debrie, C. Boulbe, and B. Faugeras, Fusion Eng. Des. **86**, 544 (2011).
[7]O. Barana, G. Manduchi, A. Murari, and JET EFDA Contributors, "Recent reactor applications of artificial neural networks to fusion plasma diagnosing and control," European Fusion Development Agreement No. EFDA-JET-PR(03)22, 2003.
[8]L. Allen and C. M. Bishop, Plasma Phys. Controlled Fusion **34**, 1291 (1992).
[9]L. Makili, J. Vega, S. Dormido-Canto, I. Pastor, and A. Murai, Fusion Eng. Des. **86**, 1213 (2011).
[10]B. Widrow and M. Lehr, Proc. IEEE **78**, 1415 (1990).
[11]D. MacKay, *Information Theory, Inference and Learning Algorithms* (Cambridge University Press, 2003).
[12]X. Garbet and R. E. Waltz, Phys. Plasmas **3**, 1898 (1996).
[13]C. -X. J. Feng, A. C. Gowrisankar, A. E. Smith, and Z. -G. S. Yu, J. Manuf. Syst. **25**, 239 (2006).
[14]M. Hagiwara, IEICE Trans. Inf. Syst. **E78-D**(8), 1080 (1995).
[15]D. E. Rumelhart, G. E. Hinton, and R. J. Williams, Nature **323**, 533 (1986).
[16]W. W. Pfeiffer, R. H. Davidson, R. W. Miller, and R. E. Waltz, "ONETWO: A computer code for modeling plasma transport in tokamaks," General Atomics Report No. GA-A16178, 1980.
[17]R. E. Waltz, J. C. DeBoo, and M. N. Rosenbluth, Phys. Rev. Lett. **65**, 2390 (1990).
[18]O. Meneghini and L. Lao, Plasma Fusion Res. **8**, 2403009 (2013).
[19]S. Nissen, Department of Computer Science University of Copenhagen Report DIKU-31, 2003.